ACS OMEGA

Open Access

http://pubs.acs.org/journal/acsodf

Article

New Perspective on Hydrogen Bonding

John F. Wager*

Cite This: *ACS Omega* 2023, 8, 41674−41679

Read Online

ACCESS | Metrics & More | Article Recommendations

ABSTRACT: A new model is proposed for hydrogen bonding in which an intermediate hydrogen atom acts as a bridge bond connecting two adjacent atoms, X and A, via quantum mechanical tunneling of the hydrogen electron. A strong hydrogen bond (X−H−A) is formed when the X−H and H−A interatomic distances are short and symmetric, thereby facilitating intense electron tunneling to and from both adjacent atoms. The hydrogen bond weakens (X−H···A) as the H···A interatomic distance lengthens compared to that of X−H since the H···A tunneling intensity degrades exponentially with increasing distance. Two modes of electron tunneling are distinguished. When an electron tunnels from H to either X or A (forward tunneling), the X−H···A bond is initially charge neutral but after tunneling is charged as either X^-−H^+···A or X−H^+···A^-. In contrast, electron tunneling from either X^- or A^- back to H^+ (reverse tunneling) discharges the X−H···A bond, resetting it back into its neutral charge state. Reverse tunneling is central to understanding the nature of a hydrogen bond. When the H···A interatomic distance is sufficiently short, reverse tunneling occurs through a triangular energy barrier (Fowler−Nordheim tunneling) such that the reverse tunneling probability is almost 100%. Increasing the H···A interatomic distance leads to a decreasing H···A reverse tunneling probability, as tunneling occurs through an asymmetric trapezoidal energy barrier (direct tunneling) until finally the H···A interatomic distance is so large that the bond persists indefinitely in the X−H^+···A^- charge state such that it is incapable of acting as a bridge bond linking X and A.

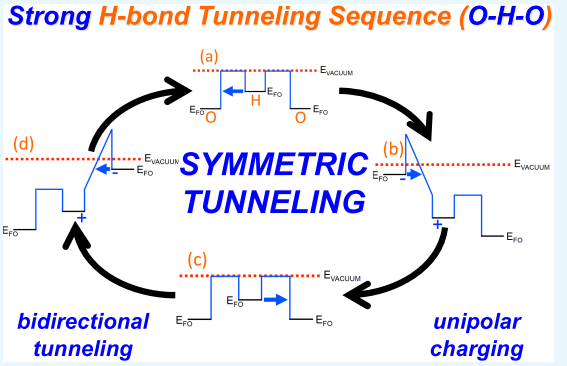

INTRODUCTION

"There is no universal agreement on the best description of the nature of the forces in the hydrogen bond."[1] Thus, discussing hydrogen bonding is an inherently hazardous undertaking.

According to the "classical" picture of hydrogen bonding,[1−6] a hydrogen bond is usually a weak bond (∼0.1−0.4 eV/bond)[2] that is formed in conjunction with two very electronegative atoms (usually F, O, or N) in which one of the electronegative atoms (X) is positioned closer to the intermediate hydrogen atom (H) than the other atom (A), such that an asymmetric X−H···A bond is formed. Weak, asymmetric X−H···A hydrogen bond examples include O−H···O (d_{O-H} = 100 pm; $d_{H\cdots O}$ = 170 pm), O−H···F (d_{O-H} = 100 pm; $d_{H\cdots F}$ = 170 pm), O−H···N (d_{O-H} = 90 pm; $d_{H\cdots N}$ = 190 pm), and O−H···Cl (d_{O-H} = 90 pm; $d_{H\cdots Cl}$ = 220 pm).[1] However, this weak, asymmetric picture of a hydrogen bond is in complete disagreement with the F−H−F hydrogen bond since it is both strong (∼2.5 eV/bond)[2] and symmetric (d_{F-H} = 120 pm; d_{H-F} = 120 pm).[1] And yet both weak, asymmetric as well as strong, symmetric bonds involving hydrogen are classified as hydrogen bonds.

A "modern" view of hydrogen bonding is more inclusive since it proposes that "there are dozens of different types of X−H···A hydrogen bonds."[6] Broadly, these hydrogen bonds can be classified as (i) strong (∼0.7−1.7 eV/bond) due to covalent bonding with $d_{X-H} \approx d_{H\cdots A}$, (ii) moderate (∼0.2−0.7 eV/bond) due to mostly electrostatic bonding with $d_{X-H} < d_{H\cdots A}$, or (iii) weak (<∼0.2 eV/bond) due to electrostatic/dispersive bonding with $d_{X-H} \ll d_{H\cdots A}$.[6] Although "modern" approaches for classifying hydrogen bonding are more liberal than "classical" approaches, most "modern" hydrogen bond definitions are formulated to exclude certain bonds involving hydrogen from consideration. For example, Steiner's requirement that "X−H acts as a proton donor to A" allows exclusion of B−H−B as a hydrogen bond,[6] while Shriver and Atkins' definition that "a hydrogen bond consists of an H atom between atoms of more electronegative nonmetallic elements" disallows B−H−B because B is not more electronegative than H, and also W−H−W since W is a metal.[5]

The goal of this contribution is to propose a new model for hydrogen bonding in which quantum mechanical tunneling of the hydrogen electron to and from adjacent X and A atoms constitutes a bridge linking these atoms to create an X−H···A hydrogen bond. This proposed hydrogen model is an extension

Received: August 10, 2023
Revised: October 5, 2023
Accepted: October 10, 2023
Published: October 26, 2023

https://doi.org/10.1021/acsomega.3c05838
ACS Omega 2023, 8, 41674−41679

of previous work in which it was asserted that covalent, ionic, and polar covalent bonding all rely on quantum mechanical tunneling, but that the nature of tunneling is different for each type of bond.[7] Covalent bonding involves bidirectional tunneling across a symmetrical energy barrier. Ionic bonding depends upon unidirectional tunneling from a cation to an anion across an asymmetric energy barrier. Polar covalent bonding is a more complicated type of bidirectional tunneling, consisting of both cation-to-anion and anion-to-cation tunneling across asymmetric energy barriers.

RESULTS AND DISCUSSION

H_2 Bonding. Prior to tackling the more complicated case of a three-atom, heteropolar X−H···A hydrogen bond, first consider the simpler two-atom, homopolar H_2 molecular bonding situation from the perspective of tunneling by examining the covalent tunneling sequence shown in Figure 1. Prior to the onset of tunneling, the two-atom system is electrically neutral, and the tunneling barrier is symmetric and rectangular, with a frontier orbital barrier height of 13.6 eV and an equilibrium interatomic separation of 74 pm for hydrogen, as indicated in Figure 1a. Suppose an electron tunnels from the left to the right frontier orbital, as indicated by the right-going blue arrow in Figure 1a. The tunneling electron negatively charges the right frontier orbital, leaving behind a positively charged left frontier orbital, as shown in Figure 1b. Negative charging pushes the right frontier orbital upward in energy, toward the vacuum level, while positive charging moves the left frontier orbital downward, away from the vacuum level; frontier orbital separation after one-electron tunneling is $U_{\Delta q=1e^-} \approx 19.5$ eV, based on a Coulombic point charge model for electrostatic energy in which one electron is transferred across the interatomic distance, as given by $U_{\Delta q=1e^-} = 1/(4\pi\varepsilon_0 d) = 1439.42/\mathrm{d}$ eV, where ε_0 is the dielectric constant of free space, and the interatomic distance, d, is expressed in units of picometers (pm).[7] Charge separation sets up an extremely large electric field of 2.6 GV/cm, as shown by the positive sloping line in Figure 1b. The type of tunneling involved in transitioning between Figure 1a,1b is denoted as forward tunneling in which an electron tunnels from a charge neutral state (Figure 1a) to an electronically charged state (Figure 1b).

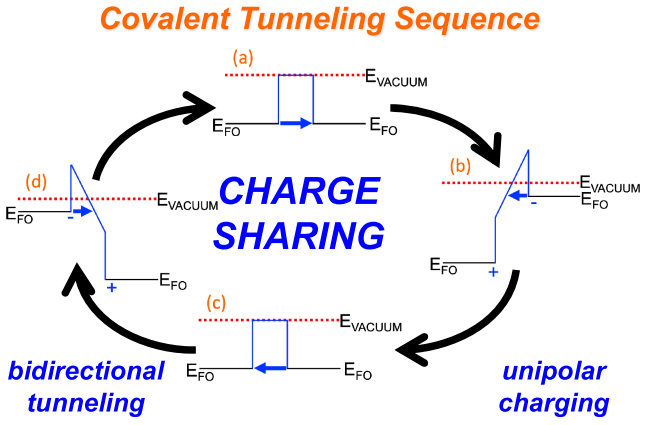

Figure 1. Homopolar (covalent) bond formation tunneling sequence for the case of molecular hydrogen, H_2. (a) An electron tunnels from the left to the right frontier orbital, leading to (b) negative (positive) charging of the right (left) frontier orbital. Next, an electron tunnels from the right to the left frontier orbital (c), neutralizing the charging such that the bond is again charge neutral. Then, an electron tunnels from the right to the left frontier orbital (d), positively (negatively) charging the right (left) frontier orbital. Finally, an electron tunnels from the left to the right frontier orbital (a), neutralizing the charging such that the bond is again charge neutral. This figure illustrates the bonding in molecular hydrogen in which it is assumed that the frontier orbital energy $E_{FO} \approx -13.6$ eV and the one-electron transfer Coulomb energy $U_{\Delta q=1e^-} \approx 19.5$ eV with an interatomic spacing of 74 pm.

In contrast, the left-going blue arrow shown in Figure 1b is an example of reverse tunneling in which an electron tunnels from and to charged frontier orbitals, thereby resetting the two-atom system back into a charge-neutral state (Figure 1c). As indicated by the left-going blue arrow of Figure 1b, this reverse tunneling process occurs through a triangular barrier of reduced thickness compared to the equilibrium interatomic distance of 74 pm; this type of tunneling through a triangle barrier of reduced thickness is termed Fowler−Nordheim tunneling.[7] Next, if an electron tunnels from the right to the left frontier orbital (left-going blue arrow in Figure 1c), positive (negative) charging pushes the right (left) frontier orbital downward (upward), as indicated in Figure 1d. Note that in Figure 1, panels (b) and (d) are similarly charged but with opposite polarities. Finally, electron tunneling (Fowler−Nordheim) from the left to the right frontier orbital (right-going blue arrow in Figure 1d) provides a reset to the neutral state (Figure 1a). As specified in Figure 1, H_2 covalent bonding involves charge sharing via bidirectional tunneling across a symmetric barrier. Bidirectional tunneling leads to bipolar charging in which frontier orbitals can be positively or negatively charged as well as neutral. The dynamic tunneling sequence shown in Figure 1 reveals that covalent bonding is Coulombic in nature due to charge separation steps of the homopolar bond formation tunneling cycle, as shown in Figure 1b,d.

Hydrogen Bonding: Qualitative. Now, we are ready to consider hydrogen bonding from a tunneling perspective. The first part of our discussion is qualitative in nature in which the tunneling dynamics of two types of three-atom, heteropolar hydrogen bonds are examined, i.e., a strong O−H−O bond and a weak O−H···O bond.

Figure 2 illustrates a tunneling sequence for a strong O−H−O hydrogen bond in which the O−H and H−O interatomic separation distances are both 120 pm. Prior to the onset of tunneling (Figure 1a), the three-atom system is electrically neutral and the tunneling barrier is asymmetric and rectangular, with hydrogen frontier orbital barrier heights of 4.5 eV and oxygen frontier orbital barrier heights of 8 eV. Suppose an electron tunnels left (forward tunneling) from the hydrogen to the left oxygen frontier orbital, as indicated by the left-going blue arrow in Figure 2a. The tunneling electron negatively charges the left oxygen frontier orbital, leaving behind a positively charged hydrogen frontier orbital, as shown in Figure 2b. Negative charging pushes the left frontier orbital upward in energy, toward the vacuum level, while positive charging moves the hydrogen frontier orbital downward, away from the vacuum level; frontier orbital separation after one-electron tunneling is $U_{\Delta q=1e^-} \approx 12.0$ eV, based on a Coulombic point charge model.[7] Charge separation sets up an extremely large electric field of -1.0 GV cm^{-1}, as shown by the steep negative sloping line in Figure 2b.

The right-going blue arrow shown in Figure 2b indicates the occurrence of Fowler−Nordheim reverse tunneling in which an electron tunnels from and to charged frontier orbitals, thereby resetting the three-atom system back into a charge-neutral state (Figure 2c). Next, an electron tunnels (forward tunneling) from

https://doi.org/10.1021/acsomega.3c05838
ACS Omega 2023, 8, 41674−41679

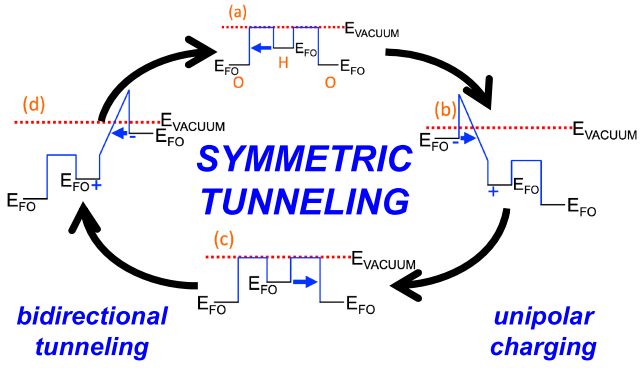

Figure 2. Strong O−H−O hydrogen bond formation tunneling sequence. (a) An electron tunnels left from hydrogen to left oxygen, leading to (b) negative (positive) charging of the left oxygen (hydrogen) frontier orbital. Next, an electron tunnels right from the left oxygen to the hydrogen frontier orbital (c), neutralizing the charging such that the bond is again charge neutral. Then, an electron tunnels right from the hydrogen to the right oxygen frontier orbital, leading to (d) negative (positive) charging of the right oxygen (hydrogen) frontier orbital. Finally, an electron tunnels left from the right oxygen to the hydrogen frontier orbital (a), neutralizing the charging such that the bond is again charge neutral. For this figure, the frontier orbital energies, $E_{FO}(H) \approx -4.5$ eV, $E_{FO}(O) \approx -8.0$ eV, and the one-electron transfer Coulomb energy, $U_{\Delta q=1e^-} \approx 12.0$ eV, with O−H and H−O interatomic spacings of 120 pm.

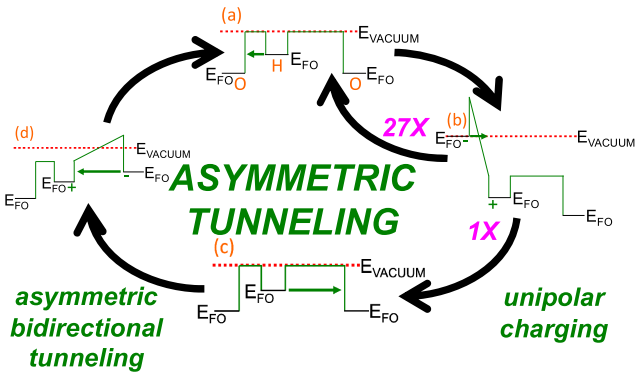

Figure 3. Weak O−H···O hydrogen bond formation tunneling sequence. (a) An electron tunnels left from hydrogen to left oxygen, leading to (b) negative (positive) charging of the left oxygen (hydrogen) frontier orbital. Next, an electron tunnels right from left oxygen to hydrogen frontier orbital, (a) or (c) neutralizing the charging such that the bond is again charge neutral. Because the O−H interatomic distance is much smaller than the H···O interatomic distance, it is 27 times more likely that charge neutralization tunneling resets to step (a) rather than step (c). When step (c) is (infrequently) accessed, an electron tunnels right from hydrogen to the right oxygen frontier orbital, leading to (d) negative (positive) charging of the right oxygen (hydrogen) frontier orbital. Finally, an electron tunnels left from right oxygen to hydrogen frontier orbital, (a) neutralizing the charging such that the bond is again charge neutral. For this figure, the frontier orbital energies $E_{FO}(H) \approx -4.5$ eV, $E_{FO}(O) \approx -8.0$ eV, and $U_{\Delta q=1e^-}$ (O−H) ≈ 16.0 eV and the one-electron transfer Coulomb energy $U_{\Delta q=1e^-}$ (H···O) ≈ 6.0 eV, with O−H and H···O interatomic spacings of 90 and 240 pm, respectively.

the hydrogen to the right oxygen frontier orbital (right-going blue arrow in Figure 2c), and positive (negative) charging pushes the hydrogen (right oxygen) frontier orbital downward (upward), as indicated in Figure 2d, setting up a positive electric field of 1.0 GV cm^{-1}. Note that in Figure 2, panels (b) and (d) are similarly charged but with opposite polarities. Finally, electron tunneling (Fowler−Nordheim reverse tunneling) from the right oxygen to the hydrogen frontier orbital (left-going blue arrow in Figure 2d) provides a reset back to the three-atom neutral state (Figure 2a). As specified in Figure 2, strong hydrogen bonding of the O−H−O involves symmetric, bidirectional tunneling across asymmetric energy barriers. In contrast to the H_2 bonding case, bidirectional tunneling in O−H−O leads to unipolar charging in which the hydrogen cation frontier orbital is neutral or positively charged, whereas oxygen anion frontier orbitals are neutral or negatively charged. The dynamic tunneling sequence illustrated in Figure 2 shows that the O−H−O bond is Coulombic in nature due to charge separation steps of the heteropolar bond formation tunneling cycle, as shown in Figure 2b,2d.

Figure 3 depicts a tunneling sequence for a weak O−H···O hydrogen bond in which the O−H and H···O interatomic separation distances are 90 and 240 pm, respectively. Prior to the onset of tunneling (Figure 3a), the three-atom system is electrically neutral and the tunneling energy barrier is asymmetric and rectangular, with hydrogen frontier orbital barrier heights of 4.5 eV and oxygen frontier orbital barrier heights of 8 eV. If an electron tunnels left (forward tunneling) from the hydrogen to the left oxygen frontier orbital, as indicated by the left-going green arrow in Figure 3a, the tunneling electron negatively charges the left oxygen frontier orbital, leaving behind a positively charged hydrogen frontier orbital, as shown in Figure 3b. Negative charging pushes the left frontier orbital upward in energy, toward the vacuum level, while positive charging moves the hydrogen frontier orbital downward, away from the vacuum level; frontier orbital separation after tunneling is $U_{\Delta q=1e^-} \approx 16.0$ eV, based on a Coulombic point charge model.[7] Charge separation sets up an extremely large electric field of −1.8 GV/cm, as shown by the negative sloping line in Figure 3b.

The right-going green arrow shown in Figure 3b indicates the occurrence of Fowler−Nordheim reverse tunneling, in which an electron tunnels from and to charged frontier orbitals, thereby resetting the three-atom system back into a charge-neutral state, corresponding to either Figure 3a or c. Because the O−H interatomic distance is much smaller than the H···O interatomic distance, it is 27 times more likely that charge neutralization tunneling resets to step (a) rather than step (c). If the reset is to step (c), then the subsequent step involves electron tunneling (forward tunneling) from the hydrogen to the right oxygen frontier orbital (right-going green arrow in Figure 3c), in which positive (negative) charging pushes the hydrogen (right oxygen) frontier orbital downward (upward), as indicated in Figure 3d; frontier orbital separation after tunneling is $U_{\Delta q=1e^-} \approx 6.0$ eV, based on a Coulombic point charge model.[7] Charge separation sets up an electric field of 0.7 GV cm^{-1}, as shown by the positive sloping line shown in Figure 3d. Note that in Figure 3d, the magnitudes of frontier orbital separation and electric field (i.e., 6.0 eV and 0.7 GV cm^{-1}) are much smaller than the corresponding Figure 3b values (16.0 eV and −1.8 GV cm^{-1}) due to the fact that the interatomic separations differ (i.e., 90 pm for O−H and 240 pm for H···O). Additionally, notice that the reverse tunneling energy barrier is trapezoidal with a thickness equal to the full equilibrium interatomic distance for Figure 3d,

https://doi.org/10.1021/acsomega.3c05838
ACS Omega 2023, 8, 41674−41679

whereas it is triangular with a reduced thickness for Figure 3b; the tunneling probability through a trapezoidal energy barrier (this type of tunneling is denoted as direct tunneling) is much smaller than the tunneling probability through a triangular energy barrier of reduced thickness (Fowler−Nordheim tunneling), as discussed below. Finally, electron tunneling (reverse direct tunneling through a trapezoidal energy barrier) from the right oxygen to the hydrogen frontier orbital (left-going green arrow in Figure 3d) provides a reset back to the three-atom neutral state (Figure 3a). As specified in Figure 3, the O−H···O hydrogen bonding involves asymmetric, bidirectional tunneling across barriers of asymmetric thickness. In contrast to the H_2 bonding case but similarly to the O−H−O hydrogen bonding case, bidirectional tunneling in the O−H···O leads to unipolar charging in which the hydrogen cation frontier orbital is neutral or positively charged, whereas oxygen anion frontier orbitals are neutral or negatively charged. The dynamic tunneling sequence shown in Figure 3 shows that the O−H···O bond is Coulombic in nature due to charge separation steps of the heteropolar bond formation tunneling cycle, as shown in Figure 3b,3d.

As a final note to this section, one subtle but potentially confusing aspect of the energy band diagrams shown in Figures 2 and 3 merits clarification. In modeling three-atom hydrogen bonds, it is assumed that both oxygen atoms bond only to the intermediate hydrogen atom. This results in floating boundary conditions in which the barrier between hydrogen and the uncharged oxygen atom does not change. Thus, the uncharged frontier orbital floats up or down with respect to the vacuum level, depending on the charge state of the hydrogen atom. The important point here is that a voltage drop occurs only with charge separation. For example, in Figure 2b, there is a voltage drop between the left oxygen atom and hydrogen because of tunneling-induced charge separation; however, there is no voltage drop between hydrogen and the right oxygen atom since there is no charge separation between these atoms. Obviously, if either or both oxygen atoms are bonded to other atoms besides the intermediate hydrogen atom, the energy band electrostatic situation is more complicated, as boundary conditions involve all bonded atoms.

Hydrogen Bonding: Quantitative. Quantitative aspects of the hydrogen bond tunneling behavior are explored. Three examples are presented, providing evidence that hydrogen bonding is mediated by quantum mechanical electron tunneling.

Table 1 lists the tunneling probabilities and mechanisms for each step of the tunneling sequences shown in Figures 2 and 3 for strong and weak O−H−O hydrogen bonds, respectively. Forward and reverse tunneling are characterized by charging or discharging of two atoms within the three-atom hydrogen bond. As evident from Table 1, forward tunneling is always a direct tunneling process involving an asymmetric rectangular barrier. In contrast, three different reverse tunneling mechanisms can be distinguished. For a strong O−H−O hydrogen bond, reverse tunneling is accomplished in both steps (b) and (d) by Fowler−Nordheim tunneling through a triangular energy barrier of reduced thickness; the tunneling probability for Fowler−Nordheim tunneling is always very large, approaching one. In contrast, for a weak O−H···O hydrogen bond, reverse tunneling occurs via Fowler−Nordheim tunneling for the shorter O−H bond of step (b) and by direct tunneling through an asymmetric trapezoidal energy barrier for the longer H···O hydrogen bond of step (d). Comparing strong O−H−O and weak O−H···O hydrogen bond tunneling behavior as summarized in Table 1, symmetry is the key critical difference between these two types of bonds; tunneling behavior is strikingly symmetric for the case of a strong O−H−O hydrogen bond, whereas it is notably asymmetric for a weak O−H···O hydrogen bond.

Table 1. Summary of Tunneling Behavior for a Strong O−H−O Hydrogen Bond with $d_{O-H} = d_{H-O}$ = 120 pm and a Weak O−H···O Hydrogen Bond with d_{O-H} = 90 pm and $d_{H\cdots O}$ = 240 pm

tunneling step[a]	tunneling probability	tunneling mechanism
strong O−H−O hydrogen bond ($d_{O-H} = d_{H-O}$ = 120 pm)		
(a)	0.042	forward, direct (asymmetric rectangular barrier)
(b)	0.987	reverse, Fowler−Nordheim (triangular barrier)
(c)	0.042	forward, direct (asymmetric rectangular barrier)
(d)	0.987	reverse, Fowler−Nordheim (triangular barrier)
weak O−H···O hydrogen bond (d_{O-H} = 90 pm, $d_{H\cdots O}$ = 240 pm)		
(a)	0.082	forward, direct (asymmetric rectangular barrier)
(b)	0.990	reverse, Fowler−Nordheim (triangular barrier)
(c)	0.003	forward, direct (asymmetric rectangular barrier)
(d)	0.002	reverse, direct (asymmetric trapezoidal barrier)

[a]Energy band diagrams for each step of the tunneling sequence for strong O−H−O and weak O−H···O hydrogen bonds are illustrated in Figures 2 and 3, respectively.

The tunneling probabilities included in Table 1 provide further confirmation of the tunneling symmetry (asymmetry) tendency of a strong O−H−O (weak O−H···O) hydrogen bond. For the strong O−H−O hydrogen bond, tunneling steps (a) and (c) have identical tunneling probabilities and mechanisms, as do steps (b) and (d). Also, the forward tunneling probability (0.042) is much smaller than the reverse tunneling probability (0.987) for a strong O−H−O hydrogen bond. This dramatic forward and reverse tunneling probability asymmetry suggests that the tunneling electron is usually found within the neutral hydrogen atom (steps (a) and (c)) and is rapidly ejected from an ionized oxygen ion when it briefly transitions through steps (b) and (d).

In contrast, for the weak O−H···O hydrogen bond shown in Table 1, all four tunneling steps have different tunneling probabilities and energy barriers (recognizing that interatomic distances differ for the asymmetric rectangular barriers of steps (a) and (c)). Although the step (a) forward tunneling probability (0.082) is small, it is much larger than the step (c) forward tunneling probability (0.003); this is a simple consequence of the 90 versus 240 pm interatomic distances associated with the O−H and H···O bonds, respectively. Differences in reverse tunneling probabilities are even more dramatic (0.990 for step (b) compared to 0.002 for step (d)). Thus, the tunneling picture that emerges for a weak O−H···O hydrogen bond is as follows. Most tunneling transitions occur back and forth between steps (a) and (b), corresponding to forward and reverse tunneling across the shorter O−H bond. Occasionally, tunneling occurs across the H···O bond. But when this happens, a very low value of the reverse tunneling probability (0.002) implies that the tunneling electron dwells persistently within the weakly bonded ionized oxygen ion prior to discharge. Persistent localization of the tunneling electron on

https://doi.org/10.1021/acsomega.3c05838
ACS Omega 2023, 8, 41674−41679

the weakly bonded ionized oxygen tends to weaken the shorter O−H bond, since less time is available for forward and reverse tunneling across the shorter O−H bond.

A few brief comments are warranted regarding how the tunneling probabilities included in Table 1 are obtained.[7] Tunneling probability across an interatomic distance of d is given by the exponential relationship $T(d) = T_0 \exp(-d/d_T)$, where T_0 is the tunneling prefactor and d_T is the characteristic tunneling distance. For an asymmetric rectangular barrier, T_0 and d_T are extracted from a best-fit regression analysis of a $T(d)$ simulation, an example of which is given in Figure 4 for

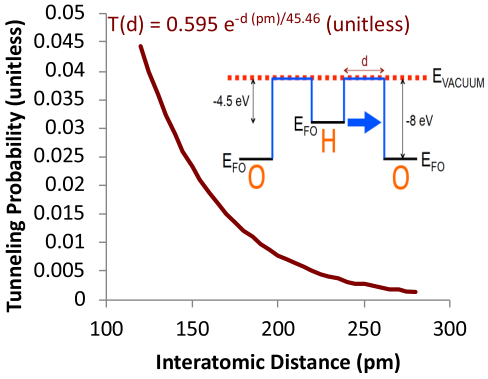

Figure 4. Tunneling probability as a function of interatomic distance, $T(d)$, for direct tunneling through an asymmetric rectangular barrier, corresponding to forward tunneling of an electron from a hydrogen frontier orbital to an oxygen frontier orbital.

tunneling between hydrogen (tunnel barrier of 4.5 eV) and oxygen (tunnel barrier of 8 eV). It is noted from Figure 4 that T_0 = 0.595 and d_T = 45.46 pm. As previously mentioned, the tunneling probability simulation indicated in Figure 4 applies to the case of an asymmetric rectangular barrier. However, this formulation is also applicable to the case of direct tunneling across an asymmetric trapezoidal barrier if the trapezoidal barrier is replaced by an equivalent asymmetric rectangular barrier.[7] Finally, Fowler−Nordheim tunneling is formulated as $T(d) = \exp(-d/d_{FN})$ such that $T_0 = 1$ and where d_{FN} is a Fowler−Nordheim characteristic tunneling distance given by $d_{FN} = 210{,}750/(V_0 + V_1)^{1.5}$ (pm) where $(V_0 + V_1)$ is equal to the energy barrier (in volts) of the X or A atom frontier orbital in a X−H···A hydrogen bond. For a complete explication of how tunneling probabilities are calculated, the interested reader is directed to ref 7.

As a second quantitative example of how the tunneling mechanism can elucidate aspects of hydrogen bonding, consider Figure 5 in which the hydrogen bond energy is plotted as a function of H···A interatomic distance, $D(d)$, in a X−H···A bond for a variety of different types of hydrogen bonds that are estimated from both experiment and theory.[8] The key takeaway from Figure 5 is that an exponential regression best-fit to the data results in a tunneling characteristic distance of 45.46 pm, identical to that obtained in the tunneling probability simulation given in Figure 4. We consider this to be strong supportive evidence that tunneling is indeed the operative mechanism underlying hydrogen bonding. Notice that a power-law fit to the data yields a slightly better coefficient-of-determination than the exponential fit, i.e., 0.94 versus 0.92. However, given the data scatter and the diverse nature of the data points included in Figure 5, we believe that there is no compelling reason to favor a power-law fit over an exponential fit.

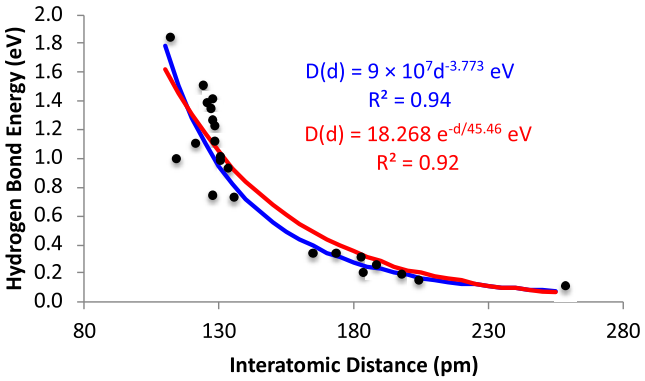

Figure 5. Hydrogen bond energy as a function of H···A interatomic distance, $D(d)$ in an X−H···A bond. Power-law (blue) and exponential (red) regression fits to the data are indicated. Data points are from Figure 2 of ref 8.

The $D(d)$ exponential fit obtained in Figure 5 is useful for classifying the nature of a given hydrogen bond. When $D \gtrsim 0.5$ eV ($d \lesssim 165$ pm), hydrogen most likely functions as a strong intramolecular bridge bond. In contrast, when $D \lesssim 0.5$ eV ($d \gtrsim 165$ pm), hydrogen likely acts as a weak intermolecular bridge bond. Interatomic distance is the key factor in establishing whether hydrogen bridging is weak or strong; this trend is a consequence of tunneling becoming more sluggish as the tunneling distance increases. It is sometimes asserted that very weak hydrogen bonds ($D \lesssim 0.2$ eV ($d \gtrsim 205$ pm)) are van der Waals bonds, involving the interaction of fluctuating dipoles.[6] We think this is unlikely and remote tunneling is more likely.

A third quantitative example of the importance of tunneling as a hydrogen bond mechanism may be developed, beginning with Figure 6. Figure 6 is an energy band diagram for an O−H···O

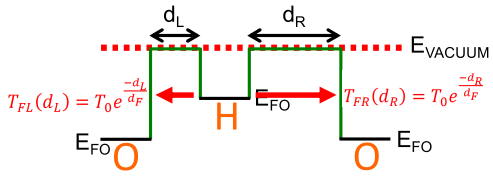

Figure 6. Energy band diagram for an O−H···O hydrogen bond. Left and right arrows indicate left- and right-directed tunneling from the hydrogen frontier orbital to the oxygen frontier orbital. Interatomic distances and tunneling parameters are subscripted L or R to denote whether they apply to the left or right energy barrier. The subscript F indicates that this is a forward tunneling process.

hydrogen bond. Tunneling parameters and interatomic distances are subscripted L or R to denote whether they apply to the left or right energy barrier with respect to the hydrogen atom. Using our exponential formulation of the tunneling probability, a charge conservation equation for the hydrogen electron can be written as

$$s_0 e^{-d_L/d_F} + s_0 e^{-d_R/d_F} = 1 \quad (1)$$

where s_0 is analogous to a tunneling prefactor but is normalized in order to ensure that charge is conserved, d_L and d_R are the left and right interatomic distances, respectively, and d_F is the characteristic forward tunneling distance; note that valence units are employed in eq 1. Equation 1 simply states that the single electron present in neutral hydrogen can tunnel either to the left or right. Normalization of s_0 is accomplished by evaluating eq 1

https://doi.org/10.1021/acsomega.3c05838
ACS Omega 2023, 8, 41674−41679

at one known d_L, d_R combination. For our strong O−H−O hydrogen bond, $d_L = d_R = 120$ pm, leading to $s_0 = 7.0$ vu assuming that $d_F = 45.46$ pm. Solving eq 1 for the left interatomic distance, d_L, results in

$$d_L = d_F \ln s_0 + d_F \ln\{1 - s_0 e^{-d_R/d_F}\} \quad (2)$$

Since s_0 and d_F are now known quantities, eq 1 establishes a quantitative link between d_L and d_R, revealing that the O−H and H···O interatomic distances are not independent of one another in an O−H···O hydrogen bond; rather, they are correlated.

Some readers may recognize the form of eq 2 as a result obtainable from bond valence theory.[9,10] In order to make this connection to bond valence theory more explicit, it is useful to introduce a change of variables, i.e., $d_L = d_{O-H}$, $d_F \ln s_0 = d_0$, $d_F = b$, and $d_L = d_{O\cdots H}$, leading to an equivalent version of eq 2 given by

$$d_{O-H} = d_0 + b \ln\left\{1 - e^{\frac{d_0 - d_{H\cdots O}}{b}}\right\} \quad (3)$$

Equation 3 is used to generate the blue and red curves for the empirical O−H and H···O bond length correlation data given in Figure 7. Two different sets of d_0, b fitting parameters are used to generate the blue and red curves of Figure 7; the blue curve is a best-fit to the data obtained by free adjustment of both d_0 and b parameters as obtained in ref 9, whereas the red fit derives from fixing $b = 45.46$ pm, and adjusting d_0 in order to obtain a best-fit to the data.

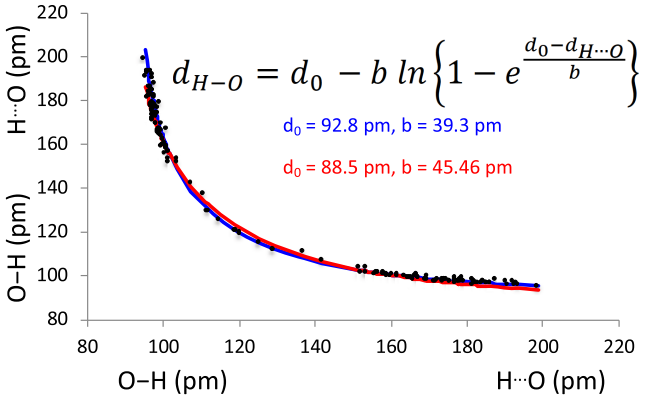

Figure 7. O−H and H···O bond length correlation. Blue and red curves are two bond valence fits to the data. Blue curve and data points are from Figure 6 of ref 9.

Two important conclusions can be drawn from Figure 7. First, both sets of d_0, b fitting parameters lead to excellent fits to the O−H and H···O bond length correlation data. This is strong supportive evidence for tunneling as the operative mechanism responsible for hydrogen bonding since eq 2 (which is equivalent to eq 3, the equation used to generate the Figure 7 curves) is derived based on three assumptions, i.e., (i) charge conservation, (ii) electron tunneling, and (iii) normalization. Second, even though both sets of d_0, b fitting parameters lead to excellent fits to the data, the blue values provide a better fit than the red fitting parameters. This suggests that the hydrogen-to-oxygen tunneling characteristic distance is closer to 39.3 pm than our previous estimate of 45.46 pm. This 15% overestimation of the characteristic tunneling distance is not surprising and is indeed quite reasonable given the abrupt, piecewise-linear approximation of the tunneling barrier shape that is used in our tunneling assessment; as previously discussed, a more realistic tunneling barrier is likely to be neither abrupt nor piecewise linear.[7] Employing the hydrogen-to-oxygen tunneling characteristic distance of 39.3 pm, the bond valence of an O−H···O hydrogen bond is given by $s_{O-H} = s_0 \exp(d_{O-H}/d_F) = \exp[(d_0 - d_{O-H})/b] = 10.6 \exp(d_{O-H}/39.3) = \exp[(92.8 - d_{O-H})/39.3]$ and $s_{H\cdots O} = s_0 \exp(d_{H\cdots O}/d_F) = \exp[(d_0 - d_{H\cdots O})/b] = 10.6 \exp(d_{H\cdots O}/39.3) = \exp[(92.8 - d_{H\cdots O})/39.3]$, where bond valence is expressed both in its exponential tunneling form, as well as its conventional Pauling format (distances are expressed in units of pm and bond valence is expressed in units of vu).

CONCLUSIONS

A new model is proposed for hydrogen bonding in which an intermediate hydrogen atom acts as a bridge bond connecting two adjacent atoms via the quantum mechanical tunneling of the hydrogen electron. Frontier orbital positioning and interatomic distances determine the tunneling intensity, which in turn establishes the hydrogen bond strength; a strong (weak) bond occurs with intense (sluggish) tunneling. The force responsible for hydrogen bonding is the Coulombic interaction associated with charge separation after forward tunneling.

AUTHOR INFORMATION

Corresponding Author

John F. Wager − *School of EECS, Oregon State University, Corvallis, Oregon 97331-5501, United States;* orcid.org/0000-0002-8992-1847; Email: jfw@eecs.oregonstate.edu

Complete contact information is available at: https://pubs.acs.org/10.1021/acsomega.3c05838

Notes

The author declares no competing financial interest.

ACKNOWLEDGMENTS

This material is based upon the work supported by the National Science Foundation under Grant No. CHE-1102637.

REFERENCES

(1) Huheey, J. E.; Keiter, E. A.; Keiter, R. L. *Inorganic Chemistry: Principles of Structure and Reactivity*, 4th ed.; Harper Collins: New York, 1993.

(2) Pauling, L. *The Nature of the Chemical Bond*, 3rd ed.; Cornell University Press: Ithaca, 1960.

(3) Pimentel, G. C.; McClellan, A. L. The Hydrogen Bond; W.H. Freeman: San Francisco, 1960.

(4) Jeffrey, G. A. *An Introduction to Hydrogen Bonding*; Oxford University Press, 1997.

(5) Shriver, D. F.; Atkins, P. W. Inorganic Chemistry, 3rd ed.; W.H. Freeman: New York, 1999.

(6) Steiner, T. The hydrogen bond in the solid state. *Angew. Chem., Int. Ed.* **2002**, *41*, 48−76.

(7) Wager, J. F.; Keszler, D. A. Bonding and tunneling. *ACS Omega* **2023**, *8*, 23182−23190.

(8) Rozenberg, M.; Loewenschuss, A.; Marcus, Y. An empirical correlation between stretching vibration redshift and hydrogen bond length. *Phys. Chem. Chem. Phys.* **2000**, *2*, 2699−2702.

(9) Steiner, T.; Saenger, W. Lengthening of the covalent O−H bond in O−H···O hydrogen bonds re-examined from low-temperature neutron diffraction data of organic compounds. *Acta Crystallogr., Sect. B: Struct. Sci.* **1994**, *B52*, 348−357.

(10) Brown, I. D. *The Chemical Bond in Inorganic Chemistry*; Oxford University Press: Oxford, 2016.

https://doi.org/10.1021/acsomega.3c05838
ACS Omega 2023, 8, 41674−41679